Cocrystallization and Phase Segregation of Polyethylene Blends between the D and H Species. 7. Time-Resolved Synchrotron-Source Small-Angle X-ray Scattering Measurements for Studying the Isothermal Crystallization Kinetics: Comparison with the FTIR Data

Kohji Tashiro,*,† Kouji Imanishi,† Yoshinobu Izumi,‡ Masamichi Kobayashi,† Katsumi Kobayashi,§ Mamoru Satoh,∥ and Richard S. Stein⊥

Department of Macromolecular Science, Faculty of Science, Osaka University, Toyonaka, Osaka 560, Japan; Macromolecular Research Laboratory, Faculty of Engineering, Yamagata University, Yonezawa, Yamagata 992, Japan; Photon Factory, National Laboratory for High Energy Physics, Tsukuba, Ibaraki 305, Japan; The Institute for Protein Research, Osaka University, Suita, Osaka 565, Japan; and Polymer Research Institute, University of Massachusetts, Amherst, Massachusetts 01003

Received March 28, 1995; Revised Manuscript Received July 3, 1995[⊗]

ABSTRACT: Time-resolved small-angle X-ray scatterings have been measured by using synchrotron radiation for the isothermal crystallization process from the melt of the blends between the fully deuterated high-density polyethylene (DHDPE) and the hydrogeneous polyethylene with various degree of ethyl branching. The crystallization rate of the pure components estimated from the time dependence of the invariant is in the order of HDPE ≫ DHDPE > LLDPE(2) ≫ LLDPE(3), where HDPE is a high-density polyethylene (PE) without branching, LLDPE(2) is a linear low-density PE with ca. 17 ethyl branches/1000 C, and LLDPE(3) is a LLDPE with ca. 41 branchings. The similar crystallization rates of DHDPE and LLDPE(2) may be one of the most important origins governing the cocrystallization behavior between the D and H species. Pairs of DHDPE/HDPE or DHDPE/LLDPE(3) show basically the phase segregation phenomena between the D and H crystalline lamellae, possibly originating from the large difference in the crystallization rate between the D and H species. It has been found that the sample of DHDPE/LLDPE(2) blend, which shows the cocrystallization phenomenon, crystallizes faster than the original pure components; i.e., an acceleration effect has been observed for the blend. On the other hand, in the cases where the D/H pair shows the phase segregation, DHDPE/HDPE and DHDPE/LLDPE(3) blends, the crystallization rate has been found to be reduced largely after blended. The crystallization rate viewed from the crystalline trans band intensity, which was measured in the time-resolved FTIR experiments, has been found to be remarkably higher than that of the invariant evaluated from the SAXS measurement. This finding supports, for the first time, experimentally the following crystallization mechanism: the trans-zigzag chain segments are generated at first from the molten random coils and then these trans segments gather together to form small crystalline clusters, which grow into larger lamellae, as detected by the small-angle X-ray scattering measurement.

Introduction

Blends between the various types of polymers have been widely investigated from the viewpoints of both industrial and scientific interests. Unfortunately, however, most of these studies have been carried out mainly by thermal analysis or through the observation of the bulk morphology. In order to clarify the relation between properties and structure of these blends more clearly, it is important to characterize the aggregation states of each component in the blends separately and from the molecular level. The blends of polyethylene (PE) with different degrees of branching must also be examined from a similar point of view. There have been reported many numbers of papers which described the morphology and melting and/or crystallization behaviors of the PE blends between high-density PE (HDPE) and low-density PE (LDPE), LDPE and linear low-density PE (LLDPE), HDPE and LLDPE, etc., through observation by optical microscopy,[1−3] electron microscopy,[4−10] DSC,[2,3,11] and small-angle light scattering.[12−16] But these techniques do not give us details on the aggregation state of the chain components in a molecular dimension. The reason may come from such a situation that the components of PE blends have the similar chemical structure of carbon and hydrogen and therefore the similar refractive indices, resulting in a small contrast for the optical measurement. One of the useful methods to trace each component separately is a use of fully deuterated species as one component. The neutron scattering cross section of deuterium is largely different from that of hydrogen, and so we can expect that the averaged radius of gyration of the D (or H) species in the molten as well as in the solid states may be estimated quantitatively through the measurement of the small-angle neutron scatterings (SANS) for the PE blend samples with various D/H contents.[17−30] Another useful method is vibrational spectroscopy. In the infrared spectra, for example, the bands intrinsic of the H and D species appear at different frequency positions, originating mainly from the difference in their atomic mass. Therefore it may be possible to trace the behavior of each species separately and simultaneously. Krimm et al. showed that, for the blend of high-density polyethylenes (HDPE) between the H and D species, the

† Department of Macromolecular Science, Osaka University.
‡ Yamagata University.
§ National Laboratory for High Energy Physics.
∥ The Institute for Protein Research, Osaka University.
⊥ University of Massachusetts.
⊗ Abstract published in *Advance ACS Abstracts,* November 1, 1995.

0024-9297/95/2228-8477$09.00/0

splitting width of the crystalline methylene bending and rocking bands reflects sensitively the spatial arrangement of these two components in the crystalline lattice.[31] On the basis of this idea, they discussed the folding structure of molecular chains in the blend sample.[32-38]

However, the results obtained from these measurements of neutron scattering and vibrational spectra are not general but are limited to the special samples obtained by quenching from the molten state. When the blend is crystallized by slow cooling from the melt, the sample tends to segregate into the two phases consisting mainly of the same kind of the component.[17] Therefore, for the samples crystallized under such normal condition as slow cooling, it is difficult to obtain the information of chains embedded in the homogeneously aggregated matrix. A few years ago, Tashiro et al. found that the blend of the deuterated HDPE (DHDPE) and the hydrogenous LLDPE with a certain degree of side chain branching shows an almost perfect cocrystallization phenomenon *even when the sample is cooled slowly from the melt* and both components coexist in the same crystalline lamella.[39-45] In this blend system, the melting temperature, the unit cell size, the interlamellar distance, the spherulite size, and so on are changed systematically and continuously with a variation in the D/H composition. At the same time, the splitting width of methylene bending and rocking bands in the IR spectra has been also observed to change systematically. On the basis of the thus obtained IR and X-ray scattering data (WAXS and SAXS), they clarified that the H and D species cocrystallize into the same crystalline lattice *in a statistically random arrangement*. In other words, the so-called random reentry folding model was proposed for the slowly cooled PE blend samples.

They also noticed another important phenomenon concerning the PE blends between the D and H species: the crystallization behavior depends largely on the degree of branching of the H species. The blends of DHDPE with the H species of much higher or lower degree of branching do not show the cocrystallization phenomenon, but they show essentially the phase segregation phenomenon. For example, in the case of the blend between DHDPE and LLDPE(2) with 17 ethyl branching/1000 carbon atoms, the almost perfect cocrystallization is observed as explained above, while for the blend between DHDPE and LLDPE(3) with ca. 41 ethyl branches, the D species begin to crystallize at first in the process of slow cooling from the melt and then the H species crystallize more slowly in a lower temperature region as the separated crystalline lamellae in a common spherulite. The blend of DHDPE with HDPE containing no side group also exhibits the phase segregation, although the phenomenon is dependent on the D/H relative content as well as on the sample preparation condition.

At this stage we have to answer the two questions: what is the factor which governs these crystallization behaviors? And what is the mixing state of chains in the melt? In order to investigate the effect of crystallization kinetics, Tashiro et al. measured the crystallization rates on the basis of the time-resolved FTIR experiments for the isothermal crystallization process from the melt.[44] It was shown that the pair of the H and D species with closer crystallization rates tends to cocrystallize together to a higher extent. This finding is quite important to understand the difference in the cocrystallization behaviors of the PE blends. As is well-known, the IR spectra are sensitive to a slight change in the local structure. In order to clarify the details of the structural change in the higher order dimension of lamellae, we need to perform, for example, the measurement of small-angle X-ray scattering (SAXS) as a function of time during the isothermal crystallization process.[46,47] In general the SAXS signals are very weak and so a long time is required to get SAXS profiles of high sound/noise ratio. The utilization of a synchrotron-source X-ray beam is considered to be quite useful for resolving this difficulty.[48,49] In this paper, the experimental data of the time-resolved SAXS measurement will be reported for a series of blends between the D and H species. The results are combined with the IR data, and the details of the crystallization behavior will be clarified from both the molecular and lamellar dimensions. As will be found in a later section, the discussion of the crystallization behavior is based on the assumption of homogeneous mixing of the chain components in the melt. The problem of this mixing will be investigated in detail in the accompanying paper[50] through the analysis of SANS data.

Table 1. Characterization of PE Samples

	M_w	M_n	M_w/M_n	branching/1000 C
DHDPE	80 000	14 000	5.7	2-3
HDPE	126 000	24 000	5.3	1
LLDPE(2)	75 000	37 000	2.0	17
LLDPE(3)	61 000	20 000	3.1	41

Experimental Section

Samples. In this study, the deuterated high-density polyethylene (DHDPE) was used as the D component in the blends, which was purchased from Merck Chemical Co., Ltd. Three kinds of linear polyethylene samples with different degrees of branching were used as hydrogenous species in blends, i.e., high-density polyethylene (HDPE) and two types of linear low-density polyethylene [LLDPE(2) and LLDPE(3)], which were supplied from Exxon Chemical Co., Ltd. For the LLDPE samples the side chain is an ethyl group. The characterization results of these samples are shown in Table 1, in which the molecular weight was evaluated using GPC and the branching content was estimated from the viscosity measurement. They were rinsed carefully by using *n*-hexane to remove the process oil. The blend samples were prepared by dissolving the H and D species of 50/50 weight ratio in boiling *p*-xylene at a concentration of 1 wt % and by precipitating into ice-methanol. Then, the samples were dried in the vacuum oven at ca. 100 °C. The samples were melted and pressed on the hot plate at ca. 150 °C and then cooled slowly to room temperature.

Time-Resolved SAXS Measurements. The SAXS measurements were performed by using the instrument installed on the beam line #10C of the Photon Factory, National Laboratory for High Energy Physics, Tsukuba, Ibaraki, Japan. The wavelength (λ) used here was 1.488 Å. The sample-to-detector distance was ca. 750 or 1900 mm. The corresponding s range was 0.002 60-0.060 00 and 0.001 04-0.029 92 Å^{-1}, respectively, and the resolution was 0.000 12 Å^{-1} in both cases, where s is a scattering vector magnitude: $s = (2/\lambda) \sin \theta$ and θ is the scattering angle. The scattered X-ray signal was detected by using a one-dimensional position sensitive proportional counter. The scattering angle was calibrated by measuring the SAXS pattern of dried-collagen as a standard.

In order to trace the crystallization process of polyethylene, which has a considerably high crystallization rate among many polymers, the temperature jump must be carried out sharply and in a stable manner. As already explained in the previous time-resolved FTIR experiments, our idea to attain this requirement was as follows. (1) The sample is jumped from the position A (the temperature higher than the melting point) to the position B (the temperature set at a predetermined

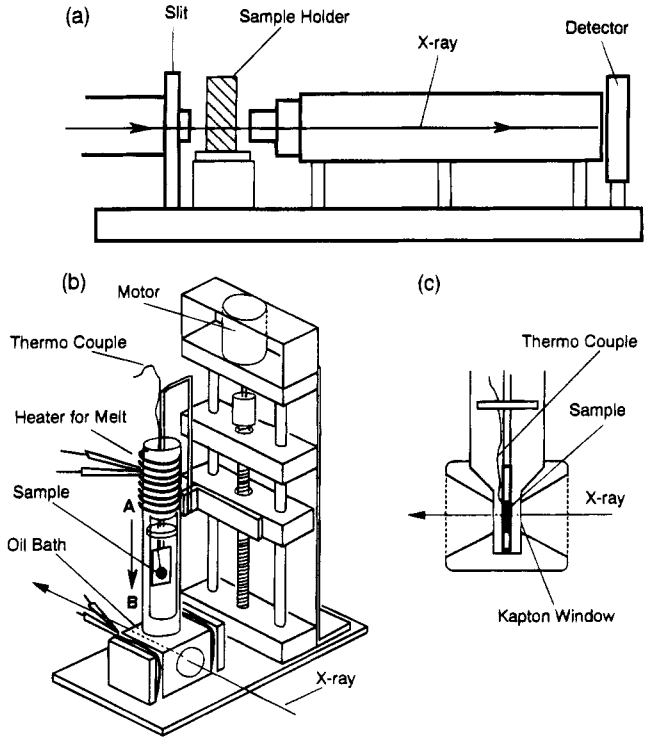

Figure 1. Schematic diagrams of (a) the SAXS equipment, (b) the temperature jump apparatus, and (c) the cross-section of the oil bath in b.

value) as rapidly as possible. (2) The temperature fluctuation, after jumping, should be diminished as much as possible by dipping the sample into a suitably temperature-controlled oil bath. (3) Air is blown up to the surface of the sample at the middle position of the jump to remove the heat on the sample surface as quickly and efficiently as possible, and (4) since nobody is allowed to enter the X-ray measurement booth, all the procedures including the jump of the sample, the temperature control, and the blowing up of the air must be regulated by remote controller. Figure 1a,b shows the schematic illustration of the X-ray diffractometer and the temperature jump apparatus. The sample of ca. 4 mm in diameter and 0.5 mm thickness was set in a metal holder. The temperature was measured directly by a thermocouple buried in the sample. Figure 1c shows the cross section of the oil bath. The pass length was designed to be as short as possible to reduce the intensity loss of the incident beam. The size of the window of the oil bath, made of polyimide film (Kapton, ca. 12.5 μm), was made as wide as possible to avoid parasitic scattering. The temperature jump was made as follows: first, the sample was melted in the metal tube of region A in Figure 1b which was heated up to a constant temperature of ca. 160 °C. Secondly, by using a motor-driven screw mechanism, the sample holder was dropped down quickly into the oil bath of region B kept at a predetermined crystallization temperature. On the way to jump from A to B, the holder was stopped for a moment and exposed to a flow of compressed air for a few seconds to remove the heat of the sample surface and then dropped into the bath. An example of temperature jump is reproduced in Figure 2. It was possible to attain the cooling rate of ca. 600 °C/min by this method with good reproducibility. In addition, the sample temperature after the jump was kept almost constant during the SAXS measurement.

The time-resolved SAXS measurement was controlled by a computer program. The measurement time was 10 or 5 s with an interval of 5 s (for the detector distance 750 mm) or 20 s without interval (for 1900 mm). The SAXS measurement was started when the sample was still in region A. The data taken during this early stage were used as a background. After a fixed time, the temperature jump was started immediately. The starting point of the crystallization was defined as the time when the sample temperature reached the predetermined value. The observed SAXS patterns were corrected by subtracting the background. The samples used for measurements were the original pure samples of the D and H species and the blend samples with D/H ratio of 50 wt %.

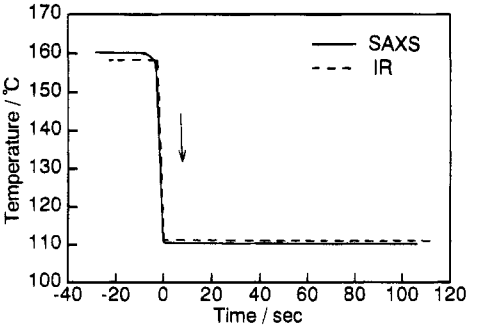

Figure 2. A comparison of temperature jump attained in the SAXS and FTIR experiments.

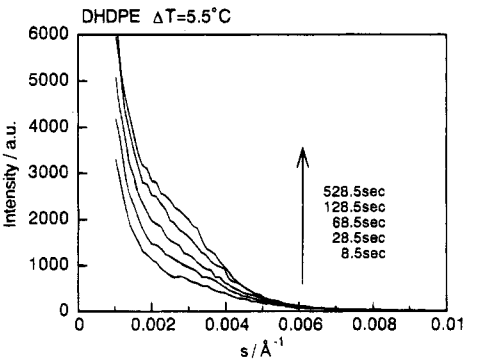

Figure 3. Time dependence of the SAXS profile measured for the pure DHDPE sample at ΔT = 5.5 °C.

DSC Temperature-Jump Measurements. The thermal analysis under an isothermal crystallization condition was also made by the DSC temperature jump method. The temperature in the sample chamber was fixed at a predetermined temperature. The sample was melted on the hot plate at ca. 150 °C and then moved manually into the sample chamber quickly, followed by the measurement of the calorimetric change. The apparatus used for measurements was DSC 120 (SEIKO Industry Inc., Japan).

Results and Discussion

Comparison of Crystallization Rates among Pure PE Samples. The crystallization temperature is sensitively influenced by the degree of supercooling (ΔT), where ΔT is the difference of the equilibrium crystallization temperature ($T°_c$) and an actual crystallization temperature (T_c): $\Delta T = T°_c - T_c$. Practically, the crystallization temperature determined by IR measurements in the slow cooling process was used for $T°_c$. As an example, Figure 3 shows the time dependence of the SAXS pattern taken for DHDPE during the isothermal crystallization process at ΔT = 5.5 °C. As the time passes, the intensity increases gradually and some shoulder begins to be detected around s = 0.003 Å^{-1}, which may be attributed to a long period. Figures 4 and 5 show the time dependencies of the invariant Q evaluated at various ΔT for the pure DHDPE and LLDPE(2), where $Q = 4\pi\int s^2 I(s)\, ds$. For both the samples, the Q increases more rapidly with time for larger ΔT. Under the assumption of the two-phase model constructed by the crystalline and amorphous phases, the invariant Q was expressed approximately as $Q \propto x(1 - x)$, where x is the degree of crystallinity. Therefore Q is almost proportional to the x at early stage of $x \ll 1$. Figure 6 shows the comparison of the time dependence of Q among the various samples of pure

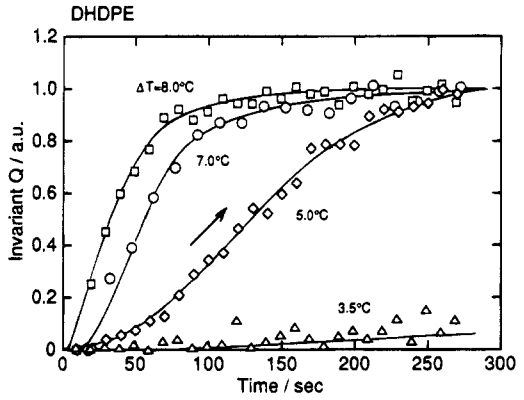

Figure 4. Time dependence of invariant Q of the pure DHDPE sample measured at the various supercoolings.

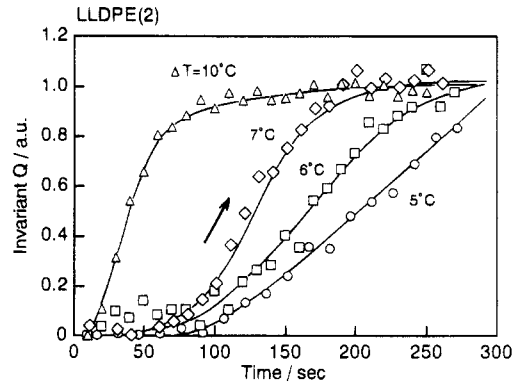

Figure 5. Time dependence of invariant Q of the pure LLDPE(2) sample measured at the various supercoolings.

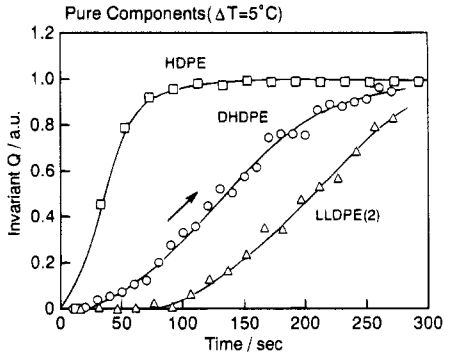

Figure 6. A comparison of the time dependence of invariant Q measured for various pure samples at $\Delta T = 5$ °C.

component ($\Delta T = 6$ °C). Figure 6 does not show the data of LLDPE(3), because it has very low crystallinity and is hard to crystallize at this ΔT. The crystallization rate is in the following order: HDPE ≫ DHDPE > LLDPE(2) ≫ LLDPE(3). This is quite consistent with the result taken from the time-resolved IR measurement. As already discussed in the FTIR experiments,[44] this order of crystallization rate is intimately related to the degree of cocrystallization. That is, DHDPE and LLDPE(2) show relatively similar crystallization rates and they exhibit an almost perfect cocrystallization phenomenon. On the other hand, the pair DHDPE/HDPE or DHDPE/LLDPE(3) shows the phase segregation phenomenon, which is related to the large difference in the crystallization rate between the D and H species. Of course, such a kinetic effect may be one of the various factors governing the complicated crystallization mechanism, but the above-mentioned parallelism between the crystallization rate and the degree of cocrystallization is not considered to be accidental but

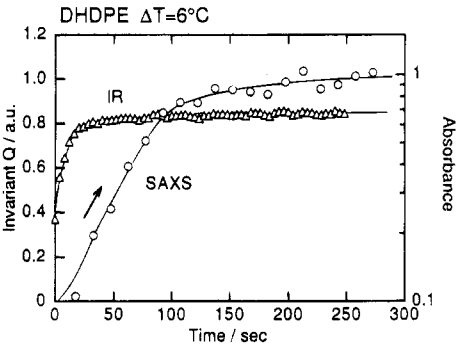

Figure 7. A comparison of crystallization behavior as detected by SAXS and FTIR measurements for the pure DHDPE sample at $\Delta T = 6$ °C.

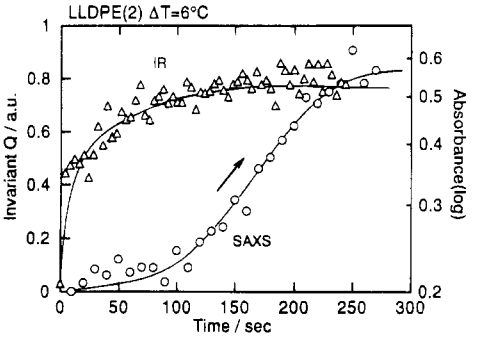

Figure 8. A comparison of crystallization behavior as detected by SAXS and FTIR measurements for the pure LLDPE(2) sample at $\Delta T = 6$ °C.

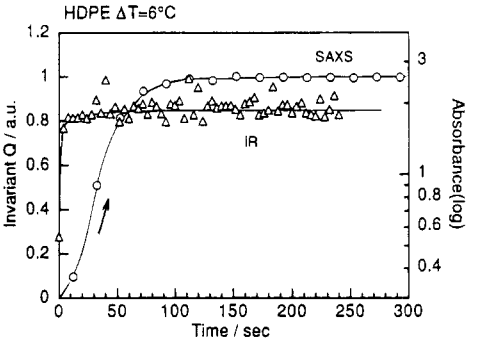

Figure 9. A comparison of crystallization behavior as detected by SAXS and FTIR measurements for the pure HDPE sample at $\Delta T = 6$ °C.

suggests some essentially important origin of the crystallization mechanism of the PE blends. As pointed out in a previous paper,[44] the thermodynamic factor should also be taken into consideration in this discussion. Even when the D and H components show similar crystallization rates, the cocrystallization may not be realized if the crystalline lattice constructed by a mixing of the D and H chains is thermodynamically unstable. In other words, the DHDPE/LLDPE(2) blend system can be said to be favored from both the kinetic and thermodynamic points of view.

Comparison between Crystallization Rates Estimated from the FTIR and SAXS Measurements. In Figures 7–9, the time dependence of Q is compared with that of the IR band intensity for the various pure samples, where the comparison between the experimental data taken from quite different sources, IR and SAXS, is possible because the temperature jump is sharp and stable in both the measurements, as illustrated in Figure 2. As shown in Figures 7–9, the increase of crystallinity measured by the IR method is

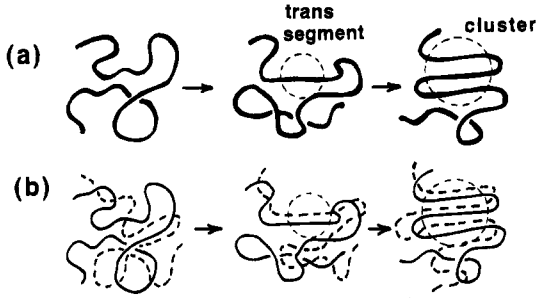

Figure 10. An illustrated crystallization mechanism of PE sample: (a) the case of pure component and (b) the case of the cocrystallized blend between the D and H species.

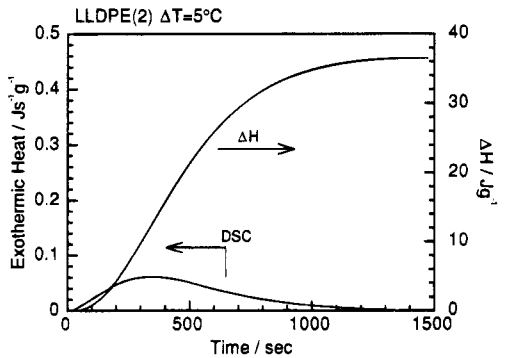

Figure 11. Time dependence of the DSC calorimetric change and the enthalpy change measured for the pure LLDPE(2) and at ΔT = 5 °C.

considerably faster than that of SAXS. This is commonly observed for all the samples. The IR spectra are considered to extract mainly the growth of the crystalline trans chains, whereas the SAXS detects the nucleation and growth of the lamellae. Therefore, the fast standing up of the IR curve and the large time lag of the SAXS data may be interpreted in the following manner. As illustrated schematically in Figure 10, at an early stage of crystallization, random-coil-like molecules transform to the ordered trans-zigzag form, where the correlation among these trans molecules is not very high. With a lapse of time, these chains begin to aggregate together to form crystalline clusters (this description is based on the observation of the growing FTIR band-splitting originated from the intermolecular interaction in the crystalline cell). These clusters grow furthermore into lamellae with a size detectable by X-ray measurement. This type of model has been speculated frequently for the crystallization mechanism of the chain molecules but without any well-defined experimental support. As seen in Figures 7–9, the organized combination of the IR and SAXS data could allow us for the first time to deduce the above-mentioned model as an experimentally established crystallization mechanism.

Comparison between DSC and SAXS Measurements. Figure 11 shows an example of temperature jump measurements by DSC. $\Delta H(t)$ is a heat of crystallization which is evaluated by integrating the DSC curve in a time region of 0 to t. Figure 12 shows the time dependence of $\Delta H(t)$ evaluated for the pure LLDPE(2) at the various ΔT: the increasing rate of $\Delta H(t)$ becomes larger with increasing supercooling, ΔT. The above-mentioned DSC data is not so accurate with respect to the time axis as compared with the other data, as understood from the difference in temperature jump techniques, but we may say roughly that the crystallization rate detected by DSC is closer to that obtained

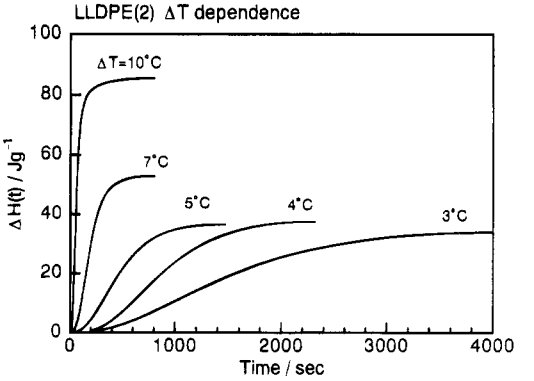

Figure 12. Time dependence of the enthalpy ΔH evaluated for the pure LLDPE(2) sample measured at the various supercoolings.

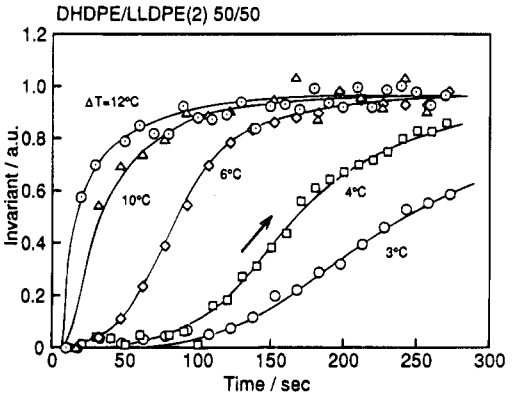

Figure 13. Time dependence of invariant Q evaluated for the DHDPE/LLDPE(2) blend sample at the various supercoolings.

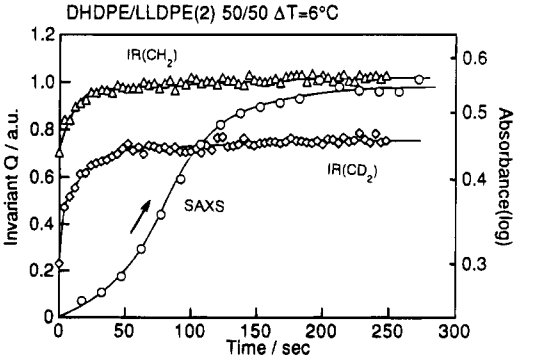

Figure 14. A comparison of the crystallization rate measured for DHDPE/LLDPE(2) blend sample between the data by SAXS and FTIR (ΔT = 6 °C).

by SAXS than that by IR. That is to say, the thermal detection can be possible for the first time when the lamella grows to a size detectable by the X-ray method, although this description might depend on the degree of sensitivity of the DSC detector.

Crystallization Rates of Blend Systems. Figure 13 shows the time dependence of Q evaluated for the DHDPE/LLDPE(2) blend system with the D/H ratio of 50/50 wt %. As likely as in the case of pure samples, the crystallization rate increases with increasing ΔT. Figure 14 shows the comparison between the SAXS and IR results. The standing up of the IR intensity occurs at an earlier stage compared with that of the SAXS intensity. This is parallel to the phenomenon observed for the pure samples. It should be noticed here that both the CH_2 and CD_2 bands increase at almost the same crystallization rate in the case of the blend sample; that is, the regular trans-zigzag segments of both the

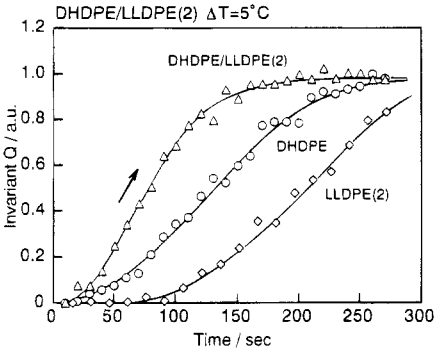

Figure 15. A comparison of the time dependence of invariant Q between the DHDPE/LLDPE(2) blend sample and the pure samples (ΔT = 5 °C).

CH_2 and CD_2 chains are considered to generate simultaneously from the melt. After a while, these trans chains gather together to form a large *cocrystallized* lamella as detected by the SAXS. In the case of DHDPE/LLDPE(3) sample, too, some of the H component crystallizes at the same rate with that of the D chain and is trapped into a lamella, although most of the H chains are still in the molten state as discussed in previous papers.[39,42] In the case of the DHDPE/HDPE blend sample, the situation is almost the same, but the roles of the D and H species are reversed: some of the D species is trapped into the HDPE lamellae.

Figure 15 shows the comparison of the crystallization rates of the pure components LLDPE(2) and DHDPE and their blend evaluated at the same ΔT. The blend sample crystallizes faster than the pure H and D components. This acceleration effect has already been detected in the time-resolved FTIR experiments. That is, both the trans-regularization of the chains, as revealed by the IR measurement, and the lamellar growth, as detected by the SAXS measurement, are accelerated in the cocrystallizable blend system. Although the true reason for this acceleration effect is not yet clarified, the energetical stabilization of the system caused by mixing of the D and H species may induce the reduction of the energy barriers for both the nucleations of trans-zigzag conformation and lamella.

Figure 16 shows the case of the DHDPE/LLDPE(3) blend sample, in which the SAXS of the pure LLDPE(3) is difficult to measure unless it is crystallized at a large ΔT. Therefore, in Figure 16a the data of the pure DHDPE and the blend sample are reproduced. Based on the time-resolved IR data (Figure 16b), the crystallization rate of the CD_2 band is reduced when the DHDPE is blended with the LLDPE(3) sample. A similar situation is recognized also in the SAXS measurement: the crystallization rate of the blend sample is lower than that of pure DHDPE sample. As reported in the following paper, the SANS measurements clarified that the D and H species are mixed together in the molten state even in this blend system. When the D component crystallizes from the melt, the D chains have to escape from the entangled network which consists of both the D and H chains. The LLDPE(3) chains act as an obstruction to this diffusional motion of the D chains, because the crystallization rate of the LLDPE(3) chain is originally lower than that of the DHDPE. As a result, a nucleation rate of the D crystal is considered to be reduced and the crystallization rate is also decreased.

Figure 17 shows the time dependence of the invariant Q evaluated for the DHDPE/HDPE blend system. Both

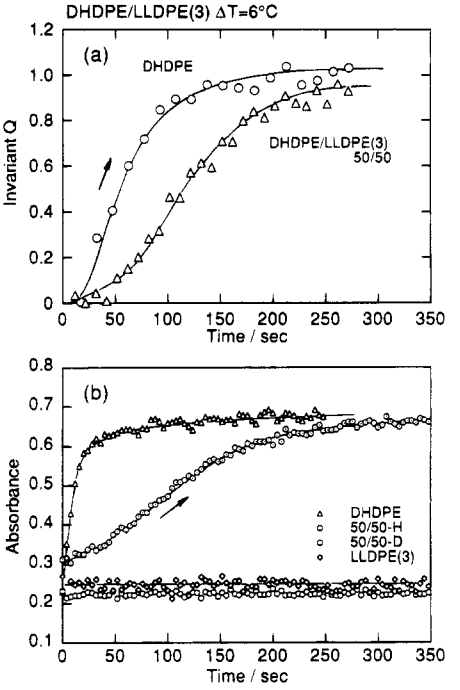

Figure 16. A comparison of the time dependence of (a) invariant Q and (b) trans-zigzag FTIR intensity between the DHDPE/LLDPE(3) blend sample and the pure samples (ΔT = 6 °C). 50/50-H: the LLDPE(3) component in the blend and 50/50-D: the DHDPE component in the blend. It is seen here that at this supercooling, the LLDPE(3) sample does not crystallize at all.

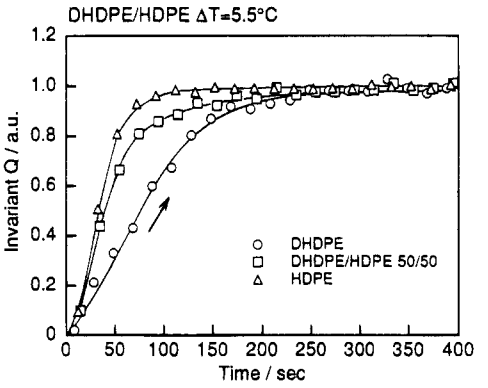

Figure 17. A comparison of the time dependence of invariant Q between the DHDPE/HDPE blend sample and the pure samples (ΔT = 5.5 °C).

the IR and SAXS data show the consistent result; the crystallization rate of the H chains is decreased and that of the D chains is accelerated. The phenomenological interpretation can also be made based on the idea discussed in the above DHDPE/LLDPE(3) case, although the role of the D and H chains should be reversed in the DHDPE/HDPE blend case, i.e., the HDPE crystallizes faster than the DHDPE.

Concluding Remarks

In this paper the time-resolved SAXS data were presented to investigate the crystallization behavior of lamellae. The results are summarized in the following way.

(1) The invariant Q was evaluated as a function of time. With an increase of the degree of supercooling (ΔT), the crystallization rate was found to increase drastically. The thus obtained results were compared with the time-resolved FTIR spectral data collected

during the isothermal crystallization with almost the same ΔT. The increasing rate of the infrared band intensity is far higher than that of the SAXS invariant, allowing us to deduce the following crystallization mechanism for the PE samples: at first the trans-zigzag chains are generated in the melt of randomly coiled chains and form small clusters. After a lapse of some time, they gather together to form larger crystalline clusters as detected by SAXS measurement. This may be the first experimental proof of the crystallization mechanism of PE viewed from the molecular level.

(2) The crystallization rates measured for the pure components of PE were compared with each other: the crystallization rate is in the order HDPE $\gg$ DHDPE > LLDPE(2) $\gg$ LLDPE(3). This suggests that the pair of the components with similar crystallization rates shows the *cocrystallization* behavior.

(3) The crystallization rate of the blends was compared with those of the pure components. In the case of the blend systems exhibiting a phase segregation phenomenon, the blend crystallizes more slowly than the pure samples. In the cocrystallizable DHDPE/LLDPE(2) case, on the other hand, the crystallization rate is rather enhanced for the blend compared with those of the pure samples, i.e., the acceleration effect was found out.

In the present SAXS measurements, the ΔT was not very large (in order to compare the SAXS data with the IR data) and the measurement was limited to the initial stage of crystallization. Therefore the peak of the long spacing of lamellae was not detected in the SAXS experiments. Measurement of the time dependence of the growing lamellar thickness may give us additional and more useful information concerning the microscopically viewed crystallization mechanism. The experimental results with larger ΔT and longer measurement time will be reported in the near future.

References and Notes

(1) Rego Lopez, J. M.; Gedde, U. W. *Polymer* **1988**, *29*, 1037.
(2) Rego Lopez, J. M.; Gedde, U. W. *Polymer* **1989**, *30*, 22.
(3) Iragorri, J. I.; Rego, J. M.; Katime, I.; Conde Brana, M. T.; Gedde, U. W. *Polymer* **1992**, *33*, 461.
(4) Barham, P. J.; Hill, M. J.; Keller, A.; Rosney, C. C. A. *J. Mater. Sci. Letter* **1988**, *7*, 1271.
(5) Rego Lopez, J. M.; Conde Brana, M. T.; Terselius, B.; Gedde, U. W. *Polymer* **1988**, *29*, 1045.
(6) Hill, M. J.; Barham, P. J.; Keller, A.; Rosney, C. C. A. *Polymer* **1991**, *32*, 1384.
(7) Hill, M. J.; Barham, P. J. *Polymer* **1992**, *33*, 4099.
(8) Hill, M. J.; Barham, P. J. *Polymer* **1992**, *33*, 4891.
(9) Conde Brana, M. T.; Gedde, U. W. *Polymer* **1992**, *33*, 3123.
(10) Rhee, J.; Crist, B. *J. Polym. Sci.: Part B: Polym. Phys.* **1994**, *32*, 159.
(11) English, A. D.; Smith, P.; Axelson, D. E. *Polymer* **1985**, *26*, 1523.
(12) Hu, S. R.; Kyu, T.; Stein, R. S. *J. Polym. Sci., B, Polym. Phys.* **1987**, *25*, 71.
(13) Kyu, T.; Hu, S. R.; Stein, R. S. *J. Polym. Sci., B, Polym. Phys.* **1987**, *25*, 89.
(14) Ree, M.; Kyu, T.; Stein, R. S. *J. Polym. Sci., Part B: Polym. Phys.* **1987**, *25*, 105.
(15) Song, H. H.; Wu, D. Q.; Chu, B.; Satkowski, M.; Ree, M.; Stein, R. S.; Phillips, J. C. *Macromolecules* **1990**, *23*, 2380.
(16) Mandelkern, L.; McLaughlin, K. W.; Alamo, R. G. *Macromolecules* **1992**, *25*, 1440.
(17) Special issue on the chain folding problem: *Faraday Discuss. Chem. Soc.* **1979**, *68*.
(18) Schelten, J.; Wignall, G. D.; Ballard, D. G. H. *Polymer* **1974**, *15*, 685.
(19) Schelten, J.; Ballard, D. G. H.; Wignall, G. D.; Longman, G. W.; Schmatz, W. *Polymer* **1976**, *17*, 751.
(20) Sadler, D. M.; Keller, A. *Polymer* **1976**, *17*, 37.
(21) Schelten, J.; Wignall, G. D.; Ballard, D. G. H.; Longman, G. W. *Polymer* **1977**, *18*, 1111.
(22) Stamm, M.; Fischer, E. W.; Dettenmaier, M. *Faraday Discus. Chem. Soc.* **1979**, *68*, 263.
(23) Nicholson, J. C.; Finerman, T.; Crist, B. *Polymer* **1990**, *31*, 2287.
(24) Banaszak, M.; Petsche, I. B.; Radozs, M. *Macromolecules* **1993**, *26*, 391.
(25) Graessley, W. W.; Krishnamoorti, R.; Balsara, N. P.; Fetters, L. J.; Lohse, D. J.; Schulz, D. N.; Sissano, J. A. *Macromolecules* **1994**, *27*, 2574.
(26) Krishnamoorti, R.; Graessley, W. W.; Balsara, N. P.; Lohse, D. J. *Macromolecules* **1994**, *27*, 3073.
(27) Balsara, N. P.; Lohse, D. J.; Graessley, W. W.; Krishnamoorti, R. *J. Chem. Phys.* **1994**, *100*, 3905.
(28) Londono, J. D.; Narten, A. H.; Wignall, G. D.; Honnell, K. G.; Hsieh, E. T.; Johnson, T. W.; Bates, F. S. *Macromolecules* **1994**, *27*, 2864.
(29) Alamo, R. G.; Londono, J. D.; Mandelkern, L.; Stehling, F. C.; Wignall, G. D. *Macromolecules* **1994**, *27*, 411.
(30) Wignall, G. D.; Londono, J. D.; Lin, J. S.; Alamo, R. G.; Galante, M. J.; Mandelkern, L. *Macromolecules* **1995**, *28*, 3156.
(31) Tasumi, M.; Krimm, S. *J. Polym. Sci., A-2* **1968**, *6*, 995.
(32) Bank, M. I.; Krimm, S. *J. Polym. Sci., A-2* **1968**, *7*, 1785.
(33) Bank, M. I.; Krimm, S. *Polym. Letter* **1970**, *8*, 143.
(34) Krimm, S.; Ching, J. H. C. *Macromolecules* **1972**, *5*, 209.
(35) Krimm, S.; Ching, J. H. C.; Folt, V. L. *Macromolecules* **1974**, *7*, 537.
(36) Ching, J. H. C.; Krimm, S. *Macromolecules* **1975**, *8*, 894.
(37) Cheam, T. C.; Krimm, S. *J. Polym. Sci., Polym. Phys. Ed.* **1981**, *19*, 423.
(38) Gregoriou, V. G.; Noda, I.; Dowrey, A. E.; Marcott, C.; Chao, J. L.; Palmer, R. A. *J. Polym. Sci., Part B: Polym. Phys.* **1993**, *31*, 1769.
(39) Tashiro, K.; Stein, R. S.; Hsu, S. L. *Macromolecules* **1992**, *25*, 1801.
(40) Tashiro, K.; Satkowski, M. M.; Stein, R. S.; Li, Y.; Chu, B.; Hsu, S. L. *Macromolecules* **1992**, *25*, 1809.
(41) Tashiro, K.; Izuchi, M.; Kobayashi, M.; Stein, R. S. *Macromolecules* **1994**, *27*, 1221.
(42) Tashiro, K.; Izuchi, M.; Kobayashi, M.; Stein, R. S. *Macromolecules* **1994**, *27*, 1228.
(43) Tashiro, K.; Izuchi, M.; Kobayashi, M.; Stein, R. S. *Macromolecules* **1994**, *27*, 1234.
(44) Tashiro, K.; Izuchi, M.; Kaneuchi, F.; Jin, C.; Kobayashi, M.; Stein, R. S. *Macromolecules* **1994**, *27*, 1240.
(45) Tashiro, K. *Acta Polym.* **1995**, *46*, 100.
(46) Schultz, J. M. *J. Polym. Sci., Part B: Polym. Phys.* **1976**, *14*, 2291.
(47) Schultz, J. M. *J. Appl. Cryst.* **1978**, *11*, 551.
(48) Song, H. H.; Stein, R. S.; Wu, D. Q.; Ree, M.; Phillips, J. C.; Legrand, A.; Chu, B. *Macromolecules* **1988**, *21*, 1180.
(49) Song, H. H.; Wu, D. Q.; Chu, B.; Satkowski, M.; Ree, M.; Stein, R. S.; Phillips, J. C. *Macromolecules* **1990**, *23*, 2380.
(50) Tashiro, K.; Imanishi, K.; Izuchi, M.; Kobayashi, M.; Itoh, Y.; Imai, M.; Yamaguchi, Y.; Ohashi, M.; Stein, R. S. *Macromolecules* **1995**, *28*, 8484 (following paper in this issue).

MA950414Q